GALEISBSTDEM: A deterministic algorithm for 1D sample by sample inversion of time-domain AEM data – theoretical details

Version 1.0, July 2015

Dr Ross. Colin. Brodie
Geoscience Australia

Australian Government

Geoscience Australia

APPLYING GEOSCIENCE TO AUSTRALIA'S
MOST IMPORTANT CHALLENGES

Contents

Contents 2
1 Introduction 3
1.1 Inversion framework 3
1.2 Coordinate system definition 4
1.3 Layered earth definition 5
1.4 System geometry definition 5
1.5 System geometry inversion 5
1.6 Reconciling primary field and system geometry 6
2 Data 7
2.1 Inversion of total or secondary field response data 7
2.2 Observed data 7
2.3 Noise 8
3 Model 8
3.1 Parameterization 8
3.2 Reference model 9
4 Forward model and derivatives 10
5 Objective function 12
5.1 Data misfit 12
5.2 Layer conductivity reference model norm 13
5.3 Layer thickness reference model norm 14
5.4 System geometry reference model norm 14
5.5 Roughness of conductivity norms 15
5.5.1 Minimization of first derivatives option 15
5.5.2 Minimization of second derivatives 16
6 Minimization scheme 16
6.1 Linearization 16
6.2 Choice of the value of λ 18
6.3 Convergence Criterion 18
7 References 19

1 Introduction

The program GALEISBSTDEM is a one dimensional (1D) deterministic inversion algorithm that can be used to invert data from most commercial time-domain airborne electromagnetic (AEM) systems including multi-moment systems. It has the capability of solving for layer conductivities, layer thicknesses, and AEM system's geometry parameters, or some subset of these.

The algorithm is described as 1D because, for the inversion of each individual AEM sample along a flight line, it uses an assumption that the Earth is horizontally stratified and has laterally-constant layer conductivities and thicknesses. This allows a simpler 1D solution to Maxwell's electromagnetic equations to be used in the modelling. It is only after 'stitching' together the entire set of conductivity models resulting from the inversion of each individual AEM sample that a pseudo-3D conductivity model is built up.

The program has options to use either a multi-layer smooth-model formulation, in which the layer thicknesses are kept fixed and only the layer conductivities are solved for, or a few-layer blocky-model formulation where both the layer conductivities and thicknesses are solved for. The inversion problem is non-unique and therefore both reference model and conductivity roughness constraints can be applied to regularize the inversion results.

The non-linear inversion problem is solved by a linearized gradient-based, iterative downhill minimization scheme. The algorithm is deterministic, meaning that, for each program run or execution, it is concerned with finding only a single optimal solution given the imposed regularization constraints for each airborne sample.

The program is parallelized via two different mechanisms. The first is the Message Passing Interface (Message-Passing-Interface-Forum, 1994), which is known as MPI. The second is Open Multi-Processing (Dagum and Menon, 1998), which is also known as OpenMP. Although they are distinctly different mechanisms, unfortunately MPI and OpenMP are often confused.

Technical information on how to run the program is detailed in the user manual (Brodie, 2015). The program is available as open-source code in an online software repository (https://github.com/GeoscienceAustralia/ga-aem.git). A time-domain AEM forward modelling program and a stochastic reversible-jump Markov Chain Monte Carlo inversion program, which endeavours to find an ensemble of solutions, are also available in the same online software repository.

1.1 Inversion framework

Figure 1 shows the overall framework under which the inversion of a single airborne sample is carried out. The elements of the figure are progressively described in the sections that follow.

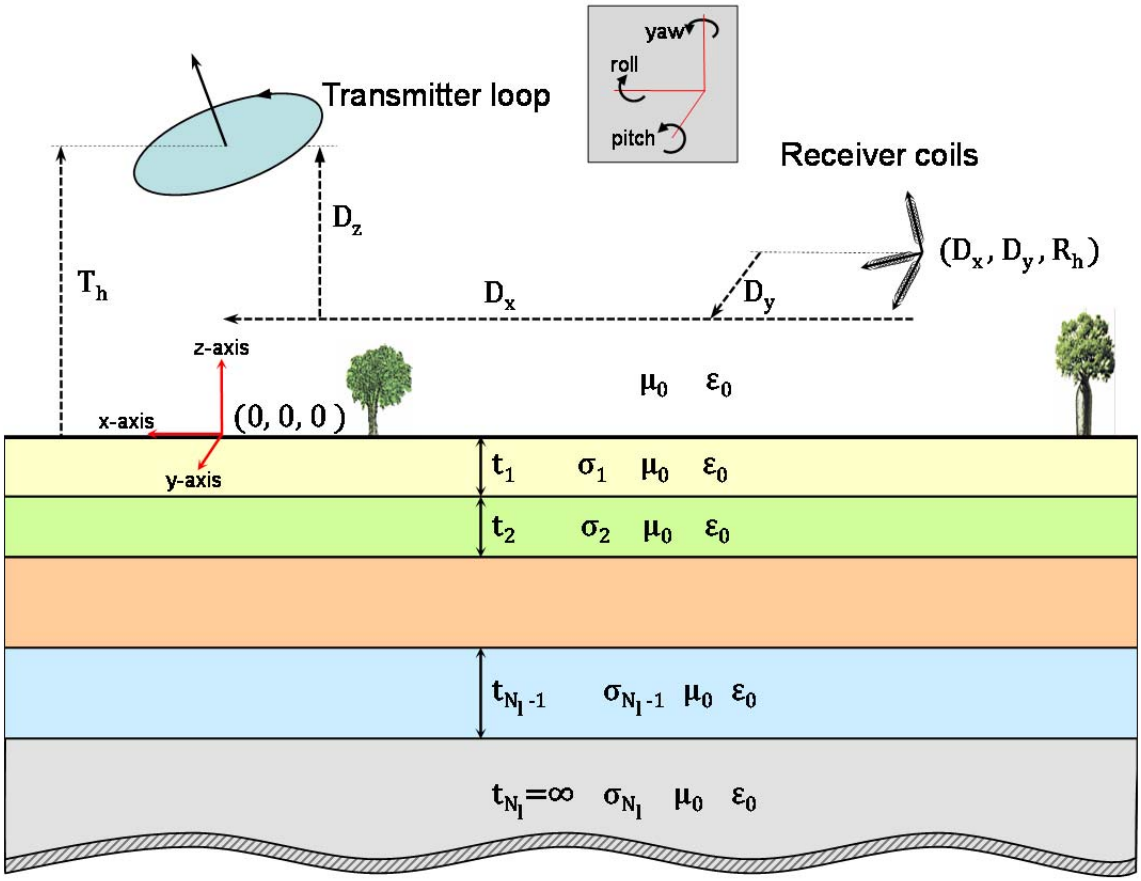

Figure 1 Schematic representation of the inversion framework for GALEISBSTDEM.

1.2 Coordinate system definition

Since each sample is inverted separately the origin of the coordinate system is different for the inversion of each sample. A right handed xyz Cartesian coordinate system is used. The origin of the coordinate system is on the Earth's surface directly below the centre of the transmitter loop. The x-axis is in the direction of flight of the aircraft at that sample location, the y-axis is in the direction of the left wing and the z-axis is directed vertically upwards.

The coordinate systems used in each individual AEM system are usually different. Therefore one must be careful to ensure the sign convention of the input electromagnetic and auxiliary data are consistent with the conventions described herein. For example, AEM data supplied by service providers generally adopts the convention where the Z-component secondary field data are positive in sign and that a positive transmitter loop pitch indicates a nose-up attitude. This is opposite to the conventions used by the GALEISBSTDEM program, and accordingly they must be sign-flipped before being used in the inversion program. Note however, that for convenience there is a mechanism for doing this built into the program.

1.3 Layered earth definition

The layered earth model is independent at each inverted sample location. The layered earth consists of N_l horizontal layers stacked on top of each other in layer cake fashion. The kth layer has thickness t_k and the bottom layer is a halfspace that has infinite thickness ($t_{N_l} = \infty$). The electrical conductivity of the kth layer is denoted σ_k and it is constant throughout that layer. The magnetic permeability of all layers is assumed to be equal to the magnetic permeability of free space μ_0. The dielectric permittivity of all layers is assumed to be equal to the permittivity of free space ε_0.

1.4 System geometry definition

The centre of the transmitter loop is located at $(0, 0, T_h)$. The position of the receiver coils relative to the transmitter loop is defined by the transmitter to receiver horizontal-inline separation (D_x), the transmitter to receiver horizontal-transverse separation (D_y), and the transmitter to receiver vertical separation (D_z), The receiver coils are thus located at (D_x, D_y, $R_h = T_h + D_z$). Note that, for a fixed-wing towed-bird system, D_x and D_z will thus be negative values.

The roll of the transmitter loop (T_r) is defined as anti-clockwise rotation, about an axis through (0, 0, T_h) and parallel to the x-axis, so that a positive roll will bring the left side of the loop upward. Pitch of the transmitter loop (T_p) is defined as anti-clockwise rotation, about an axis through (0, 0, T_h) and parallel to the y-axis, so that positive pitch will bring the front of the transmitter loop downward. Yaw of the transmitter loop (T_y) is defined as anti-clockwise rotation, about an axis through (0, 0, T_h) and parallel to the z-axis, so that a positive yaw would turn the loop toward the left. However since the x-axis is defined to be in the direction of flight at each sample, the transmitter loop yaw is always zero by definition.

The receiver coils' roll (R_r), pitch (R_p) and yaw (R_y) have the same rotational convention as for the transmitter loop except that they are rotations about the receiver coils' position (D_x, D_y, R_h).

1.5 System geometry inversion

The program has the functionality to invert for parameters of the system geometry that may not be very easily measured or estimated. This is most likely to be the case for fixed-wing systems where the towed-receiver bird is distant to the aircraft and it is logistically difficult to accurately measure its attitude and position relative to the transmitter (Smith, 2001b). The functionality can however be used for helicopter systems if the system geometry is not fully measured.

It is never particularly desirable to invert for system geometry parameters because AEM inversion is ambiguous (non-unique) enough without adding extra unknowns into the mix. However, we have found that when inverting data from fixed-wing platforms it is often impossible to fit data, to the expected noise levels, when inverting both X- and Z-component data simultaneously. It is usually possible to fit the X- or Z-component

data in two independent inversions, but only to find that the two conductivity models are systematically different, which then raises the question of which of the two models should be used. For fixed-wing systems that employ full-waveform recording and processing, a particular problem arises because of the intertwined problem of estimating the primary field and system geometry. That problem can be aided by inversion of total (primary plus secondary) field data and is discussed in detail in Section 1.6,

Even for off-time helicopter systems, there may be circumstances where it is necessary to invert for unknown elements of the system geometry. Examples would be where vegetation causes large errors in altimeter data or where altimeter and orientation instruments (e.g., gyroscopes or tilt meters) are not mounted on the transmitter/receiver assembly. Though not optimal, the system geometry inversion option can be used on the secondary field data, without the need to invert total field data. This should only be used if there are genuine reasons to believe and evidence to show that the system geometry data are incorrect and are not allowing the AEM data to be fitted to the expected noise levels with reasonable conductivity models.

For an off-time system, in which all the receiver windows are recorded when the transmitter is turned off, and has an accurately known system geometry there is no problem— we may simply use the measured system geometry to forward model the secondary field and invert the solely secondary field response data and do not need to concern ourselves with the primary or total fields.

1.6 Reconciling primary field and system geometry

Uncertain knowledge of the system geometry is intertwined with uncertain knowledge of the primary field, because if the system geometry was known accurately the primary field at the towed-receiver bird could be calculated accurately. We are not particularly interested in the primary field or the system geometry since they tell us nothing about subsurface conductivity. Nevertheless, the system geometry is required for forward modelling and hence inversion of the secondary field response, which does inform us about the subsurface.

For systems where the geometry is not explicitly measured, on-time primary field responses may be used to estimate the receiver position under certain assumptions about subsurface conductivity and the orientation of the receiver. However at survey altitude the AEM system actually measures a combined total (primary plus secondary) field response. The total field must be separated into its primary and secondary parts before the primary can be used to estimate a corresponding system geometry. But there is a conundrum because the primary cannot be isolated without the unknown system geometry and the primary cannot be isolated without the unknown subsurface conductivity. Therefore service providers have to estimate the system geometry and primary field using a certain set of assumptions. These assumptions are different for each system. See Smith (2001a); Lane *et al.* (2000), and (Leggatt *et al.*, 2000) for informative discussions on this issue.

An alternative way to deal with this conundrum is to simultaneously invert total field data for a conductivity model as well as the unknown parameters of the system geometry. This in turn implies a different, inversion derived, estimate of the primary field. This functionality is built into the algorithm and it has been widely used for the inversion of TEMPEST data (e.g., Roach, 2012) and to some extent SPECTREM data (e.g., Ley-Cooper and Brodie, 2013). However, please note that the functionality for inverting total field data in this way can only be applied to AEM system data where the data are equivalent square-wave B-field data.

2 Data

2.1 Inversion of total or secondary field response data

The user may elect to invert either secondary field or total (primary plus secondary) field response data. Typically secondary field data would be inverted. In this case the input data for the kth window data for the three components is simply $X_k^{obs} = X_k^S$, $Y_k^{obs} = Y_k^S$ and $Z_k^{obs} = Z_k^S$, where the super script ^{S} represents the secondary field response data.

However, when inverting fixed-wing towed-bird AEM data it may be beneficial invert total field response data in an effort to reconcile the problem of isolating the primary field and estimating the system geometry, as discussed in Sections 1.6, In that case, the input data for the kth window data for the three components would be $X_k^{obs} = X^P + X_k^S$, $Y_k^{obs} = Y^P + Y_k^S$ and $Z_k^{obs} = Z^P + Z_k^S$. Here, the super script ^{P} represents the primary part of the measured response. Notice that the primary field is constant over all the secondary field windows and accordingly this option is only suitable for the inversion of data from the equivalent square-wave systems (e.g., TEMPEST and SPECTREM).

If available, the primary field estimates may be explicitly input directly into the program via the input data file. However in the case that the primary field estimates were not delivered by the service provider it may be possible to reconstructed them within the program. This is provided that a set of system geometry parameters, consistent with the previously removed primary field estimates, are known or delivered with the data.

2.2 Observed data

The input data are the N_w windows of the X-, Y-, and Z-component data or any selected N_c-component subset of these. The data for the kth window are denoted X_k^{obs}, Y_k^{obs} and Z_k^{obs} for the three possible components. In general the observed data vector is of length $N_d = N_c \times N_w$ and is,

$$\mathbf{d}^{obs} = \left[X_1^{obs}, X_2^{obs}, \cdots X_{N_w}^{obs} \,\middle|\, Y_1^{obs}, Y_2^{obs}, \cdots Y_{N_w}^{obs} \,\middle|\, Z_1^{obs}, Z_2^{obs}, \cdots Z_{N_w}^{obs}\right]^T \quad (1)$$

where ^{T} represents the vector and matrix transpose operator, and $|$ indicates the possible (optional) concatenation of a subgroup of elements depending on the program options selected.

For AEM systems with multiple transmitter moments (e.g., SKYTEM) the data from each of the moments are simply concatenated together. In this case it is assumed that the measurements for each moment were recorded at the same position and with the same system geometry. It is the task of the user to **suitably** interpolate (outside of the program) the data of each moment and system geometry to new hypothetical common positions.

2.3 Noise

Errors or noise in the data are assumed to be uncorrelated and Gaussian distributed. They represent the estimated standard deviations of the Gaussian error distribution for each window and receiver component. If X_k^{err}, Y_k^{err} and Z_k^{err} represent the estimated standard deviation of the error in the kth window datum of the three components, then the data error vector, of length N_d is,

$$\mathbf{d}^{\mathrm{err}} = \left[X_1^{\mathrm{err}}, X_2^{\mathrm{err}}, \cdots X_{N_w}^{\mathrm{err}} \mid Y_1^{\mathrm{err}}, Y_2^{\mathrm{err}}, \cdots Y_{N_w}^{\mathrm{err}} \mid Z_1^{\mathrm{err}}, Z_2^{\mathrm{err}}, \cdots Z_{N_w}^{\mathrm{err}}\right]^{\mathrm{T}} \quad 2$$

The errors on the data may be calculated outside of the program and be explicitly input into the program, for every sounding and window, via the input data file.

Alternatively the errors may be calculated inside the program from the parameters of an additive plus multiplicative noise model (Green and Lane, 2003). In this model the standard deviation noise estimate for the cth component, sth sample and wth window is,

$$d_{cws}^{\mathrm{err}} = \sqrt{\left(0.01 \times p_c \times d_{cws}^{\mathrm{obs}}\right)^2 + a_{cw}^2} \quad 3$$

where p_c is the standard deviation of the percentage multiplicative error distribution assigned to all windows in the cth component, d_{csw}^{obs} is the observed secondary field data for the cth component, wth window and sth sample, and, a_{cw} is the standard deviation of the additive noise assigned to the cth component and wth window.

3 Model

3.1 Parameterization

The unknown model parameter vector $\mathbf{m}$ to be solved for in the inversion is comprised of layer conductivity parameters ($\mathbf{m}_c$), possibly layer thickness parameters ($\mathbf{m}_t$) and possibly system geometry parameters ($\mathbf{m}_g$).

The user may elect to use a multi-layer smooth-model formulation (e.g., Constable *et al.*, 1987) or a few-layer blocky-model formulation (e.g., Sattel, 1998). In the smooth-model formulation the N_l conductivities ($\sigma_1, \sigma_2, \ldots, \sigma_{N_l}$) of the layers are treated as unknowns and are allowed to vary. The N_{l-1} layer thicknesses ($t_1, t_2, \ldots, t_{N_{l-1}}$) are inputs into the algorithm, but are kept fixed throughout. In the blocky-model formulation both the conductivities and thickness are allowed to vary.

In both cases, to maintain positivity of the layer conductivities and thicknesses we actually solve for the base-10 logarithms of the conductivities and thicknesses of each layer. The vector of N_l conductivity parameters is,

$$\mathbf{m}_c = \left[\log \sigma_1 , \log \sigma_2 , \ldots \log \sigma_{N_l}\right]^T, \quad 4$$

and the vector of $N_l - 1$ thickness parameters is,

$$\mathbf{m}_t = \left[\log t_1 , \log t_2 , \ldots \log t_{N_l-1}\right]^T. \quad 5$$

In principal it is possible to solve for all ten of the system geometry parameters. However we would usually only solve for a subset of $N_g \leq 3$ system geometry parameters: In general it is not desirable to invert for system geometry parameters if they are accurately enough measured. This is because AEM inversions are already non-unique enough, without adding additional unknowns into the problem. However, as discussed in Section 1.5, in some cases it is difficult to avoid. For example, if transmitter loop altimeter data are absent or particularly noisy owing to vegetation, it may be desirable to invert for the transmitter height above ground (T_h). Also we may need to solve for some unmeasured parameters of the system geometry in fixed-wing AEM surveys as discussed in Section 1.6. In this case, it is often necessary to solve for the transmitter-receiver horizontal-inline separation (D_x), the transmitter-receiver vertical separation (D_z), and the pitch of the receiver coil assembly (R_p).

So far, the program has only really been tested on the above mentioned geometry parameters, so we will write the vector of geometry related parameters as,

$$\mathbf{m}_g = \left[T_h \mid D_x \mid D_z \mid R_p\right]^T. \quad 6$$

The complete unknown model parameter vector of length N_p to be solved for is the concatenated vector of base-10 logarithms layer conductivities, base-10 logarithms thicknesses (if using a few-layer formulation) and the geometry parameters (if solving for system geometry), so that,

$$\mathbf{m} = \left[\mathbf{m}_c \mid \mathbf{m}_t \mid \mathbf{m}_g\right]^T. \quad 7$$

3.2 Reference model

The algorithm uses the concept of a reference model (Farquharson and Oldenburg, 1993) to incorporate prior information from downhole conductivity logs or lithologic/stratigraphic logging in order to improve inversion stability and to reduce the trade-off between parameters that are not well resolved independently. Since prior information is not available everywhere within the survey area, and the inversions are carried out in independent sample by sample fashion, it is not plausible to place hard reference model constraints on the model parameters. Instead the reference model provides a 'soft' or probabilistic constraint only.

Suppose that from prior information it is concluded that the likely distribution of the model parameter m_k is a Gaussian distribution with mean m_k^{ref} and standard deviation m_k^{unc}, then the reference model vector is defined as,

$$\mathbf{m}^{ref} = \left[(\log \sigma_1)^{ref}, \ldots (\log \sigma_{N_l})^{ref} | \ldots (\log t_{N_l-1})^{ref} | T_h^{ref} | D_x^{ref} | D_z^{ref} | R_p^{ref}\right]^T, \quad 8$$

and the reference model standard deviation of uncertainty vector as,

$$\mathbf{m}^{unc} = \left[(\log \sigma_1)^{unc}, \ldots (\log \sigma_{N_l})^{unc} | \ldots (\log t_{N_l-1})^{unc} | T_h^{unc} | D_x^{unc} | D_z^{unc} | R_p^{unc}\right]^T. \quad 9$$

Note that the uncertainty of conductivities and thicknesses are defined in in base-10 logarithm units. The reference model mean values and uncertainties are inputs to the inversion algorithm and they may be different from sample to sample. The uncertainty values assigned to the reference model control the amount of constraint that the reference model places on the inversion results. A large uncertainty value for a particular parameter implies that the assigned reference model mean value is not well known and thus, all other things being equal, is allowed to vary a long way from the mean. On the other hand a low uncertainty implies the parameter is well known.

4 Forward model and derivatives

The forward model is the non-linear multi-valued function,

$$\boldsymbol{f}(\mathbf{m}) = \left[f_1(\mathbf{m}, \mathbf{p}), f_2(\mathbf{m}, \mathbf{p}), \cdots f_{N_d}(\mathbf{m}, \mathbf{p})\right]^T, \quad 10$$

which for a given a set of model parameters (**m**) calculates the theoretical B or dB/dt magnetic field data equivalent to that which would be produced for the AEM system data being inverted, after measurement and transformation by the data processing steps. The details of the AEM system configuration, units, and modelling are controlled by a user specified AEM system description file described in the user manual (Brodie, 2015).

Each $f_k(\mathbf{m}, \mathbf{p})$ is a function, not only of the layer conductivities and system geometry parameters in the inversion model parameters (**m**), but also of several other fixed auxiliary parameters (**p**) that are not being solved for (e.g., layer thicknesses in a multi-layer formulation; transmitter height, pitch and roll; receiver roll and yaw, transmitter to receiver horizontal transverse separation; system waveform and window positions etc.).

The implementation of Equation 10 is based upon the formulation of (Wait, 1982) in which he develops the frequency-domain expressions for the magnetic fields due to vertical and horizontal magnetic dipole sources above a horizontally layered medium. The formulation does not account for the contribution due to displacement currents. We also assume that effects of dielectric permittivity and magnetic susceptibility are negligible compared to electrical conduction, and set each layer's dielectric permittivity and magnetic permeability to that of free space ($\varepsilon_k = \varepsilon_0$ and $\mu_k = \mu_0$).

Details of the 1D electromagnetic modelling are provided in Brodie (2010) A summary of the procedure used for computing a time-domain system response is as follows:

i) The transmitter's current waveform (or the processed data equivalent waveform in the case of systems like TEMPEST or SPECTREM) is digitised to produce a transmitter current time series w_t.

ii) A Fast Fourier Transform (FFT) is used to compute its discrete frequency spectrum $W_f = \mathcal{F}(w_t)$.

iii) A set of logarithmically spaced discrete frequencies, lf, are determined at which the frequency-domain B-field responses are to be computed. The number of logarithmically spaced frequencies at which the expensive magnetic field calculations need to be made depends on the system bandwidth and the desired accuracy. Essentially, one must use a sufficient density of frequencies to enable accurate spline representation of the continuous frequency spectrum from the discrete samples. Six frequencies per decade are typically required to be computed over four to five decades (Raiche, 1998).

iv) The frequency-domain expressions of Wait (1982) are used to compute the magnetic B-field response B_{lf} at the receiver due to magnetic dipole(s) $M = M_0 e^{-i\omega t}$, oscillating at angular frequency $\omega = 2\pi f$, In general, for an arbitrarily oriented transmitter loop and receiver coil assembly, this requires the computation of all three orthogonal magnetic field components at the receiver coils' position for both a vertical and horizontal magnetic dipole source.

v) From the logarithmically spaced set of responses, B_{lf}, spline interpolation is used to generate a set of linearly spaced responses, B_f, at the same discrete frequencies that exist in the frequency spectrum of the waveform (W_f).

vi) Depending on whether a magnetic b-field or db/dt response is required, compute $b_t = \mathcal{F}^{-1}(B_f W_f G_f)$ or $db_t/dt = \mathcal{F}^{-1}(-i\omega B_f W_f G_f)$ by inverse FFT to yield the response time series; The term G_f represents optionally applied low-pass Butterworth filter(s) to emulate filters in the receiver system electronics.

vii) The time series b_t or db_t/dt are binned into N_w windows to simulate the AEM system's windowing method, via box-car, linear taper, or area under the curve windowing functions, to yield the required time-domain window response.

viii) Normalizations and unit conversions are applied to the window responses to appropriately simulate any such adjustments made to the acquired data being simulated.

The inversion also requires the partial derivatives of $\boldsymbol{f}(\mathbf{m})$ with respect to the model parameters (see Equation 34). These partial derivatives are all calculated analytically and their derivations are detailed in Brodie (2010). For computation of Wait's coefficient $\mathcal{R}_0$, the matrix propagation method (Farquharson *et al.*, 2003) is used because it is efficient for computation of the partial derivatives with respect to the multiple layer conductivities.

5 Objective function

The algorithm minimizes an overall objective function,

$$\Phi = \Phi_d + \lambda \Phi_m, \tag{11}$$

subject to the constraint,

$$\Phi_d \cong 1. \tag{12}$$

The objective function is comprised of a data misfit term Φ_d, and model norm term Φ_m, whose relative influences are weighted by a regularization parameter λ,

The model norm term,

$$\Phi_m = \alpha_c \Phi_c + \alpha_t \Phi_t + \alpha_g \Phi_g + \alpha_s \Phi_s, \tag{13}$$

is a weighted sum of four separate *L2* model norms. The terms Φ_c, Φ_t, Φ_g, quantify the difference between the inversion model parameters (unknowns) and their corresponding log-conductivity, log-thickness and system geometry reference model values respectively. The term Φ_s quantifies the roughness of the conductivity model's vertical structure. The weights on the individual model norm terms (α_c, α_t, α_g, and α_s) are chosen by the user and remain fixed throughout the iterative inversion procedure.

The overall regularization parameter λ is automatically chosen (see Section 6.2) by the algorithm. Initially λ is set to a high value and then in each non-linear iteration a line search is performed on λ to find its value so that Φ_d is reduced to a target misfit $\Phi_d^{tar} \cong 0.7$ of its value at the previous iteration. This iterative process continues until the constraint $\Phi_d \cong 1$ is satisfied, or the improvement between successive iterations is too small or the maximum number of iterations is reached.

5.1 Data misfit

The data misfit Φ_d is a *L2* measure of the discrepancy between the observed data ($\mathbf{d}^{obs}$) and the predicted data from the forward model function ($\boldsymbol{f}(\mathbf{m})$) , normalized by the assigned errors in the observed data ($\mathbf{d}^{err}$) and the number of data (N_d). It is defined as,

$$\Phi_d = \frac{1}{N_d} \sum_{k=1}^{N_d} \left[\frac{d_k^{obs} - f_k(\mathbf{m})}{d_k^{err}} \right]^2 = \left[\mathbf{d}^{obs} - \boldsymbol{f}(\mathbf{m}) \right]^T \mathbf{W}_d \left[\mathbf{d}^{obs} - \boldsymbol{f}(\mathbf{m}) \right], \tag{14}$$

where $\mathbf{W}_d$ is the $N_d \times N_d$ diagonal matrix,

$$\mathbf{W}_d = \frac{1}{N_d}\begin{bmatrix} \frac{1}{(d_1^{err})^2} & \cdots & \\ \vdots & \ddots & \vdots \\ & \cdots & \frac{1}{(d_{N_d}^{err})^2} \end{bmatrix}. \quad 15$$

5.2 Layer conductivity reference model norm

The layer conductivity reference model norm term Φ_c is a *L2* measure of the discrepancy, between the base-10 logarithmic conductivity model parameters and the corresponding reference model layer conductivity values. It is weighted by the layer thicknesses, and normalised by their reference model uncertainties, and the number of constraints (number of layers). It is defined as,

$$\Phi_c = \frac{1}{N_l}\sum_{k=1}^{N_l}\frac{t_k}{\bar{t}}\left[\frac{(\log\sigma_k)^{ref} - (\log\sigma_k)}{(\log\sigma_k)^{unc}}\right]^2 = \left[\mathbf{m}^{ref} - \mathbf{m}\right]^T \mathbf{W}_c \left[\mathbf{m}^{ref} - \mathbf{m}\right], \quad 16$$

where $\mathbf{W}_c$ is the $N_p \times N_p$ diagonal matrix,

$$\mathbf{W}_c = \frac{1}{N_l}\begin{bmatrix} \frac{(t_1/\bar{t})}{((\log\sigma_1)^{unc})^2} & & & & \\ & \ddots & & & \\ & & \frac{(t_{N_l}/\bar{t})}{\left((\log\sigma_{N_l})^{unc}\right)^2} & & \\ & & & 0 & \\ & & & & \ddots \\ & & & & & 0 \end{bmatrix}, \quad 17$$

and,

$$\bar{t} = \frac{1}{N_l}\sum_{k=1}^{N_L} t_k, \quad 18$$

is the mean layer thickness. Since the bottom layer is infinitely thick, for the purposes of this and other terms involving the thickness of the bottom halfspace layer, we set,

$$t_{N_L} = (t_{N_L-1})^2/t_{N_L-2}, \quad 19$$

so that the ratio of the thickness of the second-last to last layer is equal to ratio of the third-last to second-last layer.

5.3 Layer thickness reference model norm

The layer thickness reference model norm term Φ_t is a measure of the discrepancy, between the base-10 logarithmic layer thickness model parameters and the corresponding reference model values normalised by the number of constraints (thicknesses) and their reference model uncertainties. It is defined as,

$$\Phi_t = \frac{1}{N_l - 1} \sum_{k=1}^{N_l - 1} \left[\frac{(\log t_k)^{ref} - (\log t_k)}{(\log t_k)^{unc}} \right]^2 = \left[\mathbf{m}^{ref} - \mathbf{m} \right]^T \mathbf{W}_t \left[\mathbf{m}^{ref} - \mathbf{m} \right], \quad 20$$

where $\mathbf{W}_t$ is the $N_p \times N_p$ diagonal matrix,

$$\mathbf{W}_t = \frac{1}{N_l - 1} \begin{bmatrix} 0 & & & & & & \\ & \ddots & & & & & \\ & & \frac{1}{((\log t_1)^{unc})^2} & \cdots & & & \\ & & \vdots & \ddots & \vdots & & \\ & & \cdots & & \frac{1}{\left((\log t_{N_l-1})^{unc}\right)^2} & & \\ & & & & & \ddots & \\ & & & & & & 0 \end{bmatrix}. \quad 21$$

5.4 System geometry reference model norm

The system geometry reference model norm term Φ_g is a *L2* measure of the discrepancy, between the system geometry model parameters and the corresponding system geometry reference model values normalised by the number of unknown system geometry parameters and their uncertainties. It is defined as,

$$\Phi_g = \frac{1}{N_g} \sum_{k=1}^{N_g} \left[\frac{g_k^{ref} - g_k}{g_k^{unc}} \right]^2 = \left[\mathbf{m}^{ref} - \mathbf{m} \right]^T \mathbf{W}_g \left[\mathbf{m}^{ref} - \mathbf{m} \right], \quad 22$$

where g_k represents the kth unknown system geometry (e.g., TX_h, D_x, D_z, or RX_p) parameter to be solved for. The matrix $\mathbf{W}_g$ is the $N_p \times N_p$ diagonal matrix,

$$\mathbf{W}_g = \frac{1}{N_g}\begin{bmatrix} 0 & & & & \\ & \ddots & & & \\ & & 0 & & \\ & & & \frac{1}{(g_1^{unc})^2} & \\ & & & & \ddots \\ & & & & & \frac{1}{\left(g_{N_g}^{unc}\right)^2} \end{bmatrix}. \quad 23$$

5.5 Roughness of conductivity norms

The vertical roughness of conductivity norm Φ_s is a measure of the roughness of the conductivity profile. The user may elect to minimize the sum of the squares of either the first or the second derivatives of the base-10 logarithm of the conductivity with respect to depth. The derivatives are approximated by the differences between the conductivities of adjacent layers, and take into account the distance between their layer centres. The effect of each layer is weighted by the layer thickness and normalised by the number of constraints.

5.5.1 Minimization of first derivatives option

To minimize the first derivative of the conductivity profile, the term is defined as,

$$\Phi_s = \frac{1}{N_l - 1}\sum_{k=2}^{N_l}\frac{t_k}{\bar{t}}\left[\frac{\log\sigma_{k-1} - \log\sigma_k}{d_{k-1,k}}\right]^2 = \mathbf{m}^T\mathbf{L}^T\mathbf{L}\mathbf{m}, \quad 24$$

where,

$$d_{i,j} = [t_i + t_j]/2, \quad 25$$

is the distance between the centres of adjacent layers,

$$\mathbf{L} = \frac{1}{N_L - 1}\begin{bmatrix} \left[\frac{-\sqrt{s_2}}{d_{12}}\right] & \left[\frac{\sqrt{s_2}}{d_{12}}\right] & & \\ & \left[\frac{-\sqrt{s_3}}{d_{23}}\right] & \left[\frac{\sqrt{s_3}}{d_{23}}\right] & \ddots \\ & & \ddots & \end{bmatrix} \quad 26$$

is a diagonal $N_l - 1 \times N_p$ matrix, and

$$s_k = \frac{t_k}{\bar{t}}. \qquad 27$$

Again, for the purposes of these terms, the thickness of the bottom layer (t_{N_l}) is set as shown in Equation 19.

5.5.2 Minimization of second derivatives

To minimize the second derivatives of the conductivity profile, the term is defined as,

$$\Phi_s = \frac{1}{N_l - 2} \sum_{k=2}^{N_l - 1} \frac{t_k}{\bar{t}} \left[\frac{\log \sigma_{k-1} - \log \sigma_k}{d_{k-1,k}} - \frac{\log \sigma_k - \log \sigma_{k+1}}{d_{k,k+1}} \right]^2 = \mathbf{m}^T \mathbf{L}^T \mathbf{L} \mathbf{m}, \qquad 28$$

where,

$$\mathbf{L} = \frac{1}{N_L - 2} \begin{bmatrix} \left[\frac{\sqrt{s_2}}{d_{12}}\right] & \left[\frac{-\sqrt{s_2}}{d_{12}} + \frac{-\sqrt{s_2}}{d_{23}}\right] & \left[\frac{\sqrt{s_2}}{d_{23}}\right] & & \\ & \left[\frac{\sqrt{s_3}}{d_{23}}\right] & \left[\frac{-\sqrt{s_3}}{d_{23}} + \frac{-\sqrt{s_3}}{d_{34}}\right] & \left[\frac{\sqrt{s_3}}{d_{34}}\right] & \\ & & \ddots & \ddots & \ddots \end{bmatrix}, \qquad 29$$

is a $N_l - 2 \times N_p$ matrix, and $d_{i,j}$ and s_k are as defined in Equations 25 and 27 respectively.

In both the first and second derivatives roughness norm terms above, the weighting/normalization by s_k, $N_l - 2$, and $N_l - 1$ is not particularly necessary. They are included just to help standardize the magnitude of the Φ_s term and thus selection of α_s) for different runs of the program, for example, if the number of layers is changed or the thicknesses are changed.

6 Minimization scheme

6.1 Linearization

To minimize the overall objective function Φ, a linearized gradient based iterative minimization scheme is used. Collection of the matrix notation parts of the objective function terms from Equations 11, 13, 14, 16, 20, 22, and 24, allows us to write,

$$\begin{aligned}\Phi(\mathbf{m}) = &\left[\mathbf{d}^{\text{obs}} - \boldsymbol{f}(\mathbf{m})\right]^{\text{T}}\mathbf{W}_{\text{d}}\left[\mathbf{d}^{\text{obs}} - \boldsymbol{f}(\mathbf{m})\right] \\ &+\lambda\alpha_{\text{c}}\left[\mathbf{m}^{\text{ref}} - \mathbf{m}\right]^{\text{T}}\mathbf{W}_{\text{c}}\left[\mathbf{m}^{\text{ref}} - \mathbf{m}\right] \\ &+\lambda\alpha_{\text{t}}\left[\mathbf{m}^{\text{ref}} - \mathbf{m}\right]^{\text{T}}\mathbf{W}_{\text{t}}\left[\mathbf{m}^{\text{ref}} - \mathbf{m}\right] \\ &+\lambda\alpha_{\text{g}}\left[\mathbf{m}^{\text{ref}} - \mathbf{m}\right]^{\text{T}}\mathbf{W}_{\text{g}}\left[\mathbf{m}^{\text{ref}} - \mathbf{m}\right] \\ &+\lambda\alpha_{\text{s}}\mathbf{m}^{\text{T}}\mathbf{L}^{\text{T}}\mathbf{L}\mathbf{m}\end{aligned} \quad 30$$

The inversion begins by setting the initial estimate of the model parameters to the reference model ($\mathbf{m}_0 = \mathbf{m}^{\text{ref}}$). During the nth iteration the current estimate of the model parameters $\mathbf{m}_{\text{n}}$ is perturbed by the parameter change vector,

$$\Delta\mathbf{m}_{\text{n}} = \mathbf{m}_{\text{n+1}} - \mathbf{m}_{\text{n}}. \quad 31$$

The forward model at the new set of model parameters $\mathbf{m}_{n+1}$ is approximated by a Taylor series expansion about $\mathbf{m}_{\text{n}}$, which, after excluding high order terms reduces to,

$$\boldsymbol{f}(\mathbf{m}_{\text{n+1}}) \approx \boldsymbol{f}(\mathbf{m}_{\text{n}}) + \mathbf{J}_{\text{n}}(\mathbf{m}_{\text{n+1}} - \mathbf{m}_{\text{n}}), \quad 32$$

where $\mathbf{J}_{\text{n}} = \partial\boldsymbol{f}(\mathbf{m})/\partial\mathbf{m}$ is the Jacobian matrix whose ith, jth element is the partial derivative of the ith datum with respect to the jth model parameter evaluated at $\mathbf{m}_{\text{n}}$ in model space.

Making use of Equation 32, and substituting $\mathbf{m} = \mathbf{m}_{\mathbf{n+1}}$, allows Equation 30 to be rewritten as,

$$\begin{aligned}\Phi(\mathbf{m}_{\text{n+1}}) = &\\ &+\left[\mathbf{d}^{\text{obs}} - \boldsymbol{f}(\mathbf{m}_{\text{n}}) - \mathbf{J}_{\text{n}}(\mathbf{m}_{\text{n+1}} - \mathbf{m}_{\text{n}})\right]^{\text{T}}\mathbf{W}_{\text{d}}\left[\mathbf{d}^{\text{obs}} - \boldsymbol{f}(\mathbf{m}_{\text{n}}) - \mathbf{J}_{\text{n}}(\mathbf{m}_{\text{n+1}} - \mathbf{m}_{\text{n}})\right] \\ &+\lambda\alpha_{\text{c}}\left[\mathbf{m}^{\text{ref}} - \mathbf{m}_{\text{n+1}}\right]^{\text{T}}\mathbf{W}_{\text{c}}\left[\mathbf{m}^{\text{ref}} - \mathbf{m}_{\text{n+1}}\right] \\ &+\lambda\alpha_{\text{t}}\left[\mathbf{m}^{\text{ref}} - \mathbf{m}_{\text{n+1}}\right]^{\text{T}}\mathbf{W}_{\text{t}}\left[\mathbf{m}^{\text{ref}} - \mathbf{m}_{\text{n+1}}\right] \\ &+\lambda\alpha_{\text{g}}\left[\mathbf{m}^{\text{ref}} - \mathbf{m}_{\text{n+1}}\right]^{\text{T}}\mathbf{W}_{\text{g}}\left[\mathbf{m}^{\text{ref}} - \mathbf{m}_{\text{n+1}}\right] \\ &+\lambda\alpha_{\text{s}}\mathbf{m}_{\mathbf{n+1}}^{\mathbf{T}}\mathbf{L}^{\text{T}}\mathbf{L}\mathbf{m}_{\text{n+1}}\end{aligned} \quad 33$$

Since the value of Φ will be minimized when $\partial\Phi/\partial\mathbf{m}_{\text{n+1}} = 0$, we differentiate Equation 33 with respect to the elements of $\mathbf{m}_{\text{n+1}}$ and setting the result to zero, we get,

$$\begin{aligned}\partial\Phi/\partial\mathbf{m}_{\text{n+1}} = 0 = &-2\mathbf{J}_{\text{n}}^{\text{T}}\mathbf{W}_{\text{d}}\left[\mathbf{d}^{\text{obs}} - \boldsymbol{f}(\mathbf{m}_{\text{n}}) - \mathbf{J}_{\text{n}}(\mathbf{m}_{\text{n+1}} - \mathbf{m}_{\text{n}})\right] \\ &-2\lambda\alpha_{\text{c}}\mathbf{W}_{\text{c}}\left[\mathbf{m}^{\text{ref}} - \mathbf{m}_{\text{n+1}}\right] \\ &-2\lambda\alpha_{\text{t}}\mathbf{W}_{\text{t}}\left[\mathbf{m}^{\text{ref}} - \mathbf{m}_{\text{n+1}}\right] \\ &-2\lambda\alpha_{\text{g}}\mathbf{W}_{\text{g}}\left[\mathbf{m}^{\text{ref}} - \mathbf{m}_{\text{n+1}}\right] \\ &-2\lambda\alpha_{\text{s}}\mathbf{m}_{\mathbf{n+1}}^{\mathbf{T}}\mathbf{L}^{\text{T}}\mathbf{L}\mathbf{m}_{\text{n+1}}\end{aligned} \quad 34$$

Cancellation of the *2s* and collecting terms in the unknown vector $\mathbf{m}_{\text{n+1}}$ on the left hand side, yields,

$$\left[\mathbf{J}_n^T\mathbf{W}_d\mathbf{J}_n + \lambda\left(\alpha_c\mathbf{W}_c + \alpha_t\mathbf{W}_t + \alpha_g\mathbf{W}_g + \alpha_s\mathbf{L}^T\mathbf{L}\right)\right]\mathbf{m}_{n+1} = \mathbf{J}_n^T\mathbf{W}_d\left[\mathbf{d}^{obs} - \boldsymbol{f}(\mathbf{m}_n) + \mathbf{J}_n\mathbf{m}_n\right] + \lambda\left[\alpha_c\mathbf{W}_c + \alpha_t\mathbf{W}_t + \alpha_g\mathbf{W}_g\right]\mathbf{m}^{ref}. \quad 35$$

which is the familiar form of a linear system of equations,

$$\mathbf{A}\mathbf{m}_{n+1} = \mathbf{b}, \quad 36$$

where,

$$\mathbf{A} = \mathbf{J}_n^T\mathbf{W}_d\mathbf{J}_n + \lambda\left[\alpha_c\mathbf{W}_c + \alpha_t\mathbf{W}_t + \alpha_g\mathbf{W}_g + \alpha_s\mathbf{L}^T\mathbf{L}\right], \quad 37$$

and,

$$\mathbf{b} = \mathbf{J}_n^T\mathbf{W}_d\left[\mathbf{d}^{obs} - \boldsymbol{f}(\mathbf{m}_n) + \mathbf{J}_n\mathbf{m}_n\right] + \lambda\left[\alpha_c\mathbf{W}_c + \alpha_t\mathbf{W}_t + \alpha_g\mathbf{W}_g\right]\mathbf{m}^{ref}. \quad 38$$

We may then solve the linear system (Equation 36) to yield $\mathbf{m}_{n+1}$ using a variety of standard linear algebra methods. We use singular value decomposition.

6.2 Choice of the value of λ

In each iteration the inversion program employs a 1D line search method to automatically select a value for the regularization parameter (λ). In the line search, Equation 36 is solved multiple times using different values of λ^{trial} to find a value such that the data misfit is reduced to approximately 0.7 of its previous value at the previous iteration, that is such that,

$$\Phi_d(\mathbf{m}_{n+1}) \approx \Phi_d^{tar} = 0.7 \times \Phi_d(\mathbf{m}_n). \quad 39$$

This follows the philosophy of Constable *et al.* (1987), and helps ensure that the data misfit is reduced slowly. If it is reduced too rapidly there is a risk that unnecessary structure will be introduced into the solution.

An additional 1D line search is also be carried out during (nested within) the solution for each value of λ^{trial} to find the step factor f such that $\Phi_d(\mathbf{m}_n + f\Delta\mathbf{m})$ is minimized on the interval $0 < f \leq 1$. This step length damping prevents the solution overshooting the minimum in the search direction $\Delta\mathbf{m}$.

The combination of these two nested 1D line search procedures is relatively computationally expensive because several (possibly several tens) of forward models are required in each iteration. While this is not preferable, it does improve the overall robustness.

6.3 Convergence Criterion

The iterations continue until the inversion terminates when one of the following conditions is encountered:

i) Φ_d reaches a user defined minimum value Φ_d^{min} (e.g., 1.0);

ii) Φ_d could not be reduced by more than a user specified percentage (e.g., 1%) in two consecutive iterations; and

iii) the user specified maximum number of iteration (e.g., 100) is reached.

7 References

Brodie, R. C., 2010. Holistic inversion of airborne electromagnetic data. Australian National University, Canberra. Ph.D. Thesis. Online: http://hdl.handle.net/1885/49403.

Brodie, R. C., 2015. User Manual for Geoscience Australia's Airborne Electromagnetic Inversion Software. Online: https://github.com/GeoscienceAustralia/ga-aem.git.

Constable, S. C., Parker, R. L. and Constable, C. G., 1987. Occam's inversion; a practical algorithm for generating smooth models from electromagnetic sounding data. *Geophysics* **52(3)**, 289-300.

Dagum, L. and Menon, R., 1998. OpenMP: an industry standard API for shared-memory programming. *Computational Science & Engineering, IEEE* **5(1)**, 46-55. doi: 10.1109/99.660313.

Farquharson, C. G. and Oldenburg, D. W., 1993. Inversion of time-domain electromagnetic data for a horizontally layered Earth. *Geophysical Journal International* **114**, 433-442.

Farquharson, C. G., Oldenburg, D. W. and Routh, P. S., 2003. Simultaneous 1D inversion of loop-loop electromagnetic data for magnetic susceptibility and electrical conductivity. *Geophysics* **68(6)**, 1857-1869.

Green, A. and Lane, R., 2003. Estimating noise levels in AEM data. *In: 16th Geophysical Conference and Exhibition*, Brisbane, Queensland, Australia, Australian Society of Exploration Geophysicists.

Lane, R., Green, A., Golding, C., Owers, M., Pik, P., Plunkett, C., Sattel, D. and Thorn, B., 2000. An example of 3D conductivity mapping using the TEMPEST airborne electromagnetic system. *Exploration Geophysics* **31**, 162-172.

Leggatt, P. B., Klinkert, P. S. and Hage, T. B., 2000. The Spectrem airborne electromagnetic system—further developments. *Geophysics* **65(6)**, 1976-1982.

Ley-Cooper, A. Y. and Brodie, R. C., 2013. Inversion of Spectrem AEM data for conductivity and system geometry. *In: 23rd International Geophysical Conference and Exhibition*, Melbourne, Victoria, Australia, Australian Society of Exploration Geophysicists. Online: http://www.publish.csiro.au/paper/ASEG2013ab145.

Message-Passing-Interface-Forum, 1994. MPI: A message-passing interface standard. *International Journal of Supercomputing Applications* **8(3-4)**, 165-416.

Raiche, A., 1998. Modelling the time-domain response of AEM systems. *Exploration Geophysics* **29(1&2)**, 103-106.

Roach, I. C. (ed), 2012. The Frome airborne electromagnetic (AEM) survey, South Australia: implications for energy, minerals and regional geology. Geoscience Australia. **Record 2012/40**, 296 pp.

Sattel, D., 1998. Conductivity information in three dimensions. *Exploration Geophysics* **29(1&2)**, 157-162.

Smith, R. S., 2001a. On removing the primary field from fixed–wing time–domain airborne electromagnetic data: some consequences for quantitative modelling, estimating bird position and detecting perfect conductors. *Geophysical Prospecting* **49**, 405–416.

Smith, R. S., 2001b. Tracking the transmitting–receiving offset in fixed–wing transient EM systems: methodology and application. *Exploration Geophysics* **32**, 14–19.

Wait, J. R., 1982. Geo-electromagnetism. Academic Press Inc, New York. 268 pp.